

LASERS

PACS numbers: 42.55.Lt; 42.60.Lh
DOI: 10.1070/QE2012v042n11ABEH014926

Study of a plate-electrode XeCl laser with a pulse repetition rate up to 5 kHz

D.D. Voevodin, A.V. Vysotskii, B.V. Lazhintsev, A.V. Pisetskaya

Abstract. **The results of the study of a repetitively pulsed XeCl laser with a high rate of pulse repetition and the electrode assembly based on a multi-section discharge gap with inductance-capacitance stabilisation of the discharge are presented. The multi-section discharge gap is formed by 25 pairs of anode–cathode plates. The discharge formed in the interelectrode gap had the dimensions 250×12×2 mm. The studies were performed using the HCl–Xe–Ne laser mixture at the total pressure up to 3.5 atm. The limit value of the radiation pulse repetition rate was equal to 5 kHz. The mean-square deviation of the pulse energy increased from 0.8% to 1.6% in the range of repetition rates from 1 to 4.5 kHz and did not exceed 2.4% at the frequency 5 kHz. The maximal energy of the laser pulse and the efficiency coefficient were equal to 7.9 mJ and 1.6%, respectively. The maximal power of laser radiation (31 W) was obtained at the repetition rate 5 kHz. A new technique of measuring the gas flow velocity in the interelectrode gap is proposed. The velocity of gas circulation at the maximal pressure of the mixture did not exceed 18 m s^{-1}. Optical inhomogeneities were observed, caused by a high concentration of electrons in the discharge plasma, by the acoustic wave, arising in the discharge gap, and by the heating of the gas in the discharge.**

Keywords: *electric-discharge XeCl laser, multi-plate electrodes, inductance-capacitance stabilisation, pulse repetition rate, radiation energy stability, shadow technique, optical inhomogeneities.*

1. Introduction

At present many technological applications (lidar systems, microlitography, material processing, etc.) require lasers operating in the UV range with a high rate of radiation pulse repetition. To date, among such lasers the excimer ones possess the highest power. The high pulse repetition rate in such lasers is achieved at the expense of reducing the width of the discharge gap and choosing the appropriate velocity of the gas flow.

In Ref. [1] the pulse repetition rate $f \approx 5$kHz was obtained in a XeCl excimer laser with the active medium volume 1220×22×10 mm at the circulation velocity $V \approx 120$ m s^{-1}. The output power in this laser amounted to 0.5 kW, while the power supplied to provide the He buffer gas circulation at the pressure 1.76 atm approached 50 kW. Increasing the radiation pulse repetition rate at the expense of increasing the gas flow velocity is associated with significant technical problems. At the velocity $V \approx 55$ m s^{-1} of active medium circulation in a XeF laser [2] with the discharge gap width 3 mm, the repetition rate $f \approx 5.5$ kHz was obtained. Using the same laser chamber, the maximal repetition rate of ~5 kHz was achieved in a KrF laser [3].

In Refs [4–6] the radiation pulse repetition rate $f \leqslant 4$–5 kHz was demonstrated in XeF and KrF lasers at a moderate gas circulation velocity ($V \leqslant 19$ m s^{-1}) in a compact laser chamber with the electrode system, based on multi-plate electrodes and inductance–capacitance discharge stabilisation. In the present paper we report the results of the study of XeCl laser operation with a similar laser chamber. Optimisation of the XeCl laser parameters is carried out, and high values of the radiation pulse repetition rate are obtained. Optical inhomogeneities are observed in the interelectrode gap, which are associated with a high concentration of electrons in the discharge plasma, with the acoustic wave, arising in the discharge gap, and with heating of the gas in the discharge volume. Shadow technique of measuring the gas flow velocity is developed.

2. Experimental results

The XeCl laser was constructed on the basis of the working chamber of the commercial CL-5000 excimer laser (Physics Instrumentation Centre, A.M. Prokhorov General Physics Institute of the Russian Academy of Sciences, Troitsk) and the electrode assembly with multi-section discharge gap, described in [4–6]. The discharge was formed in the interelectrode gap with the dimensions 250 × 12 × 2 mm. The distance between the cavity mirrors ($R_1 = 100\%$, $R_2 = 27\%$) was 50 cm. Preionisation was implemented using 25 spark discharges, located upstream the gas flow. The gas mixture circulation was provided using a diametrical blower driven by a dc electric motor via a magnetic clutch.

The circuit of the pulsed laser pump included the storage capacitor C_s (2.8 or 3.5 nF), the peaker capacitor C_p (2.35 nF) and the preionisation capacitor C_{pr} (0.5 nF). The charging of the peaker capacitor was implemented using the C–C scheme. To provide inductance–capacitance decoupling, each pair of electrode plates had its own peaker capacitor $C_p^{(i)}$ (0.094 nF) connected, which, in turn, was charged via its own decoupling inductor $L_p^{(i)}$ (1 μH) from the mutual storage capacitor [4–6]. In order to reduce the losses, arising in the thyratron in the course of recharging the capacitors, an additional inductor was included into the electric circuit of the thyratron. The optimal value of its inductance amounted to 310 nH. The peaking capacitor voltage was controlled by means of a resistive splitter, and the discharge current – by means of a planar

D.D. Voevodin, A.V. Vysotskii, B.V. Lazhintsev, A.V. Pisetskaya
Russian Federal Nuclear Centre 'All-Russian Research Institute of Experimental Physics', prosp. Mira 37, 607188 Sarov, Nizhnii Novgorod Region, Russia; e-mail: npi3@yandex.ru

Received 29 May 2012
Kvantovaya Elektronika **41** (11) 980–984 (2011)
Translated by V.L. Derbov

low-inductance shunt, the length of which was equal to the width of the discharge gap.

The HCl–Xe–Ne gas mixture served as an active medium of the laser. At the first stage of the studies the optimisation of partial pressures of the mixture components was carried out. The pressure of HCl varied within the range of 1.5–4 Torr, and the pressure of Xe within the range 15–30 Torr. With the growth of the Ne buffer gas pressure the lasing energy increases, that is why the pressures of HCl and Xe were optimised under the maximal total allowable pressure 3.5 atm in the laser chamber for all charging voltages. When optimising the HCl and Xe pressures within the above-mentioned limits, the lasing energy varied by no greater than 20%. The optimal pressure amounted to 2.3 Torr for HCl and 19 Torr for Xe. The width of the discharge region, measured using the method of Ref. [4], was equal to 2 mm for the active mixture HCl : Xe : Ne = 2.3 : 19 : 2400 Torr.

Figure 1 shows the dependences of energy and efficiency coefficient of the laser on the charging voltage for different values of the storage capacitance. At $C_s = 2.8$ nF the maximal lasing energy 7.3 mJ was achieved at the efficiency coefficient, equal to 1.1%, and the charging voltage $U = 22$ kV. The maximal efficiency coefficient (1.5%) with this capacitance was implemented at $U = 16$ kV. The increase in storage capacitance C_s from 2.8 to 3.5 nF lead to an increase in radiation energy. The maximal energy of the laser pulse amounted to 7.9 mJ at the charging voltage $U = 22$ kV.The maximal efficiency coefficient (1.6%) was observed at $C_s = 3.5$ nF and $U = 14$ kV. Within the limits $U = 16$–22 kV the increase in the storage capacitance from 2.8 to 3.5 nF caused the reduction of the efficiency coefficient by 0.1%–0.2%. A further increase in C_s without appropriate increase in C_p would probably lead to a further reduction of the efficiency coefficient.

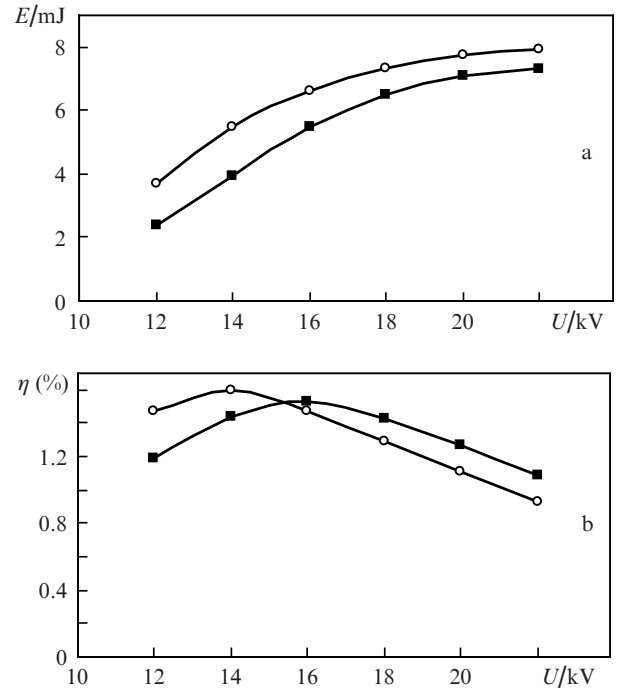

Figure 1. Dependences of the energy E (a) and the efficiency coefficient (b) of the laser on the charging voltage U. The active mixture HCl : Xe : Ne = 2.3 : 19 : 2400 Torr. The storage capacitance $C_s = 2.8$ (■) and 3.5 nF (○).

The next stage of the study was related to the investigation of the operation regime of the laser with a high pulse repetition rate. The energy of a train of laser pulses (1000 pulses) with a high repetition rate ($f \geqslant 1$ kHz) was measured with the thermocouple sensor No. 70263 (Oriel), and the energy stability of laser pulses was registered with the Nova II power and energy meter (Ophir) and the PD10 photodiode sensor, which recorded the energy of each pulse in the train.

Figure 2 presents the dependences of the laser pulse energy E and its relative mean-square deviation σ on the pulse repetition rate at the charging voltage 18 kV. From Fig. 2 it is seen that within the limits of $f = 1$–4 kHz at $C_s = 2.8$ nF the energy of radiation remains unchanged. At $f \geqslant 4$ kHz the energy significantly decreases with increasing repetition rate. The mean energy of the laser radiation pulse at $f = 5$ kHz amounted to 6.3 mJ, the mean power of radiation being equal to 31 W. At $f \leqslant 4.5$ kHz the value of σ did not exceed 1.6%, and at $f = 5$ kHz it was equal to 2.4%. In the case when $C_s = 3.5$ nF and $U = 18$ kV at $f > 4.5$ kHz the failure of the thyratron operation occurred. At the same capacitance and $U = 20$ kV the thyratron operation failure was observed already at $f > 3$ kHz. The stability of laser radiation energy from pulse to pulse did not change under the variation of the storage capacitance within the range of stable thyratron operation. The stability of laser pulse energy and the limiting rate of pulse repetition are determined by the velocity of gas circulation in the interelectrode gap, as well as by the stability of thyratron operation, which decreases under the growth of the charging voltage [6].

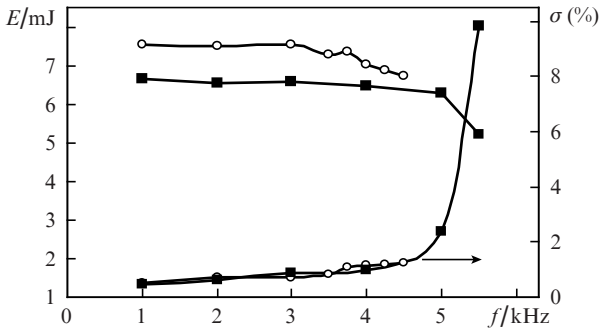

Figure 2. Dependences of the energy of lasing pulse E and its relative mean-square deviation σ on the pulse repetition rate f for a train of 1000 pulses. The active mixture HCl : Xe : Ne = 2.3 : 19 : 2400 Torr. The storage capacitance C_s=2.8 (■) and 3.5 nF (○), the charging voltage U = 18 kV.

The velocity of the gas flow in the interelectrode gap is one of the basic technical characteristics of a repetitively pulsed laser. In Ref. [5], in order to estimate the gas flow velocity, the discharge glows, excited by two successive current pulses, were fixed in a single-frame photograph. In the present paper the measurement of the gas flow velocity in the interelectrode gap was implemented using the shadow technique with photoelectric registration of the optical signal. The schematic of the experiments on measurements of the gas flow velocity is presented in Fig. 3.

In the experiments the probing beam (*2*) passed through the area, located downstream the gas flow, parallel to the optical axis of the laser chamber (*5*). Moving the beam over the discharge gap region, one can measure the gas flow veloc-

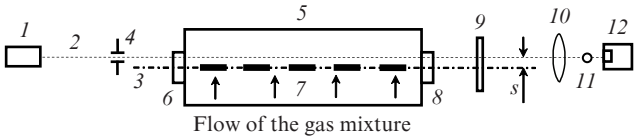

Figure 3. Optical schematic diagram of the experiment on measuring the velocity of gas flow using the shadow technique: (*1*) probing laser; (*2*) probing beam; (*3*) plane of electrodes; (*4*) aperture; (*5*) laser chamber; (*6*, *8*) cavity mirrors of the laser chamber; (*7*) electrodes; (*9*) light filters; (*10*) focusing lens; (*11*) screen; (*12*) photoelectric detector.

ity at different points near the laser electrodes. The radiation power of the probing He–Ne laser GN-15-1 was ~15 mW with the beam divergence 1.2×10^{-3} rad. The aperture (*4*) with the diameter 0.13 cm was used to fix the diameter and the divergence of the probing beam in the region under study. In the focus of the lens (*10*) (F = 5.5 cm) the screen (*11*) was mounted, consisting of a tungsten 0.007-cm-thick wire coated with carbon-black. The diameter of the first diffraction minimum of the probing beam was equal to ~0.0065 cm. The SPPD16 photoelectric sensor (*12*) with the diameter of detector area 0.25 cm was placed closely to the screen. The focused radiation did not spread beyond the aperture of the detector sensitive area, when the probing beam propagated through the region of optical inhomogeneity.

The volume of the gas heated in the discharge corresponds to an optical inhomogeneity with the length $L \sim 25$ cm, moving together with the gas flow. As a result of refraction at the optical inhomogeneity, the probing radiation in the focus of the lens is displaced by $d = FL\mathrm{grad}\,n$ and appears at the photosensitive area of the detector (*12*). A characteristic oscillogram of the signal from the photoelectric detector, induced by the probing beam, is presented in Fig. 4.

The first narrow pulse in the oscillogram is caused by the radiation of the discharge. The second narrow pulse located near the first one arises when the optical inhomogeneity created by the acoustic wave, which is excited by the discharge region expansion, crosses the probing beam. The third and the fourth broad pulses are associated with the front and back boundaries of the optical inhomogeneity, formed by the heated and expanded discharge region, drifting with the gas flow and crossing the probing beam. In the discharge region with maximal energy yield, where $\mathrm{grad}\,n \approx 0$, the probing beam does not move off the shadow screen. The distance s from the axis of the probing beam with the effective diameter ~0.86 mm to the vertical plane, passing through the optical axis of the laser chamber, equals ~3.5 mm (see Fig. 3).

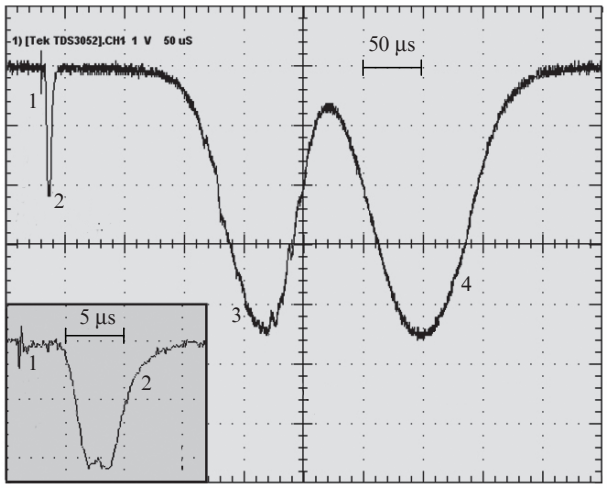

Figure 4. Oscillogram of the photoelectric detector signal. The active mixture HCl:Xe:Ne = 2.3:19:2400 Torr. The charging voltage U = 20 kV.

The duration $\Delta\tau$ of the second pulse, corresponding to the acoustic wave, amounts to ~5 µs at the level I_{max}/e. The velocity of sound in neon is equal to ~450 m s^{-1}. The acoustic wave must propagate through the distance from the interelectrode gap centre to the centre of the probing beam during the time ~7.8 µs, while the time, measured using the oscillogram, appeared to be ~6.7 µs. The difference may be explained by assuming that the expansion of the discharge volume gives rise to a weak shock wave rather than to a sound wave (the change of the volume of the heated and expanded discharge region is 7.6%). The shock wave propagates with somewhat 1.16-times greater velocity than the sound wave. During the time $\Delta\tau$ such a wave passes the distance 2.6 mm. Thus, the width of the 'sound' optical inhomogeneity is ~3 mm.

As shown in Ref. [7], the distribution of the discharge glow intensity over the cross section of the active volume practically coincides with the distribution of the energy input into the discharge plasma. Using the discharge glow intensity distribution and taking into account the isochoric plasma heating, followed by adiabatic gas expansion for realistic energy inputs, the calculations were performed to determine the gas density distribution in the region of discharge energy release. We also calculated the refractive index gradient that appears at the front and back boundaries of the optical inhomogeneity region, arising as a result of the processes considered. The maximal value of this gradient amounted to 1.3×10^{-4} cm^{-1}. The width of the thermal optical inhomogeneity, caused by the heated and expanded discharge region, was equal to ~3.3 mm. The character of the signal, recorded by the photodiode in the process of measuring the gas circulation velocity, fully corresponds to the calculated distribution of the refractive index gradient of the optical inhomogeneity. This agreement is observed both in the region of the optical inhomogeneity, caused by the acoustic wave, and in the region of gas, heated by the discharge and drifting with laser medium circulation.

The velocities of the active medium in the laser chamber in question vary depending on the height of the discharge gap within the range of 10%–15%. Figure 5 presents the velocities of the gas flow in the centre of the discharge gap, determined using the shadow method. For comparison in the same figure we present the results of measuring the gas flow velocity by single-frame photographing of discharge glows, excited by two successive pulses of current [5]. It is seen that the velocities, determined using the two methods, are practically coincident.

For each velocity of gas circulation a maximal (limiting) rate of pulse repetition exists, at which the relative mean-square deviation of the pulse energy remains acceptable ($\sigma \leqslant$ 2%). With a further increase in the repetition rate the value of begins to grow rapidly. In Fig. 6 the dependence of the limiting repetition rate on the gas circulation velocity is shown. It is practically linear. The coefficient of gas mixture purification, defined by the expression $K = Vl(fD)$ (D being the width of the discharge region), for all operating repetition rates amounted to ~1.8.

In Ref. [5] it was noticed for the first time that the refractive index gradient, caused by high concentration of free elec-

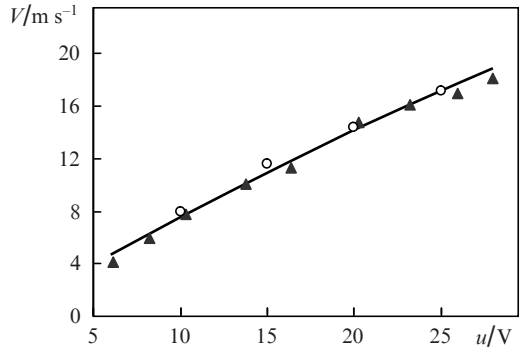

Figure 5. Dependences of the gas flow velocity V in the centre of the interelectrode gap on the ventilator drive voltage u, obtained using the shadow technique (○) and single-frame photographing of discharge glows excited by two successful pulses of the current (▲).The active mixture HCl : Xe : Ne = 2.3 : 19 : 2400 Torr.

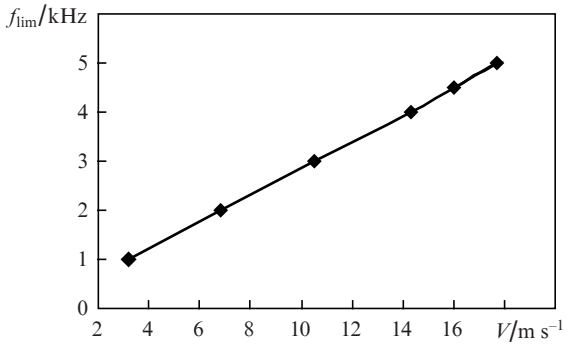

Figure 6. Dependence of the limiting pulse repetition rate f_{lim} on the velocity V of gas circulation. The active mixture HCl : Xe : Ne = 2.3 : 19 : 2400 Torr. Charging voltage U = 20 kV, storage capacitance C_s = 2.8 nF.

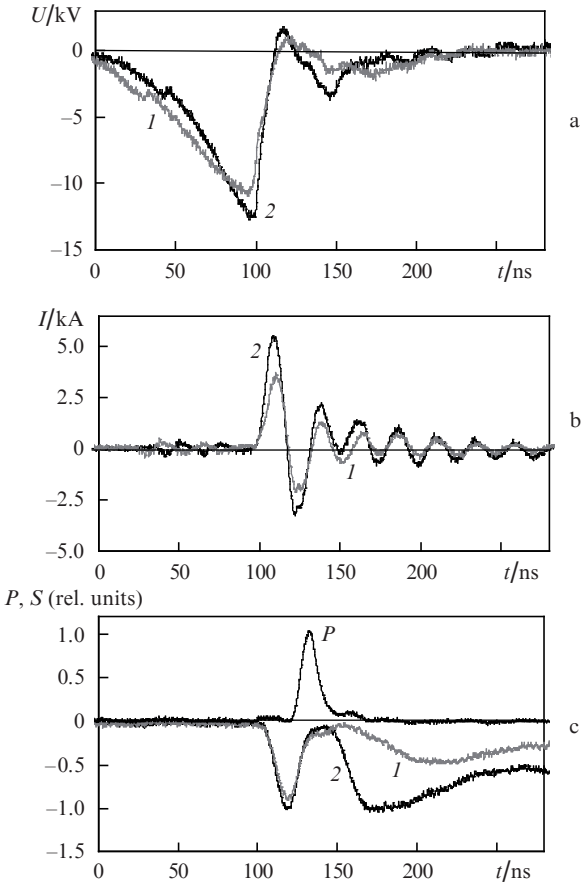

Figure 7. Oscillograms of the voltage (a) and current (b) in the discharge circuit, as well as the lasing pulse (P) and the signals S from the photoelectric detector at U = 14 (*1*) and 20 kV (*2*) (c). The active mixture HCl : Xe : Ne = 2.3 : 19 : 2400 Torr.

trons in the discharge plasma, affects the formation of laser radiation directional pattern in excimer lasers with a 'narrow' discharge. This effect leads to splitting of the laser beam in the far-field zone. In the present work similar studies were carried out with the XeCl laser, using the scheme, presented in Fig. 3, in which the face of an optical waveguide with the diameter 0.65 mm was placed in the focal plane of the lens (*10*), having greater focal length (F = 55 cm). Through this waveguide the radiation was transported to a photodiode, the signal from which after a high-frequency amplifier was registered with an oscilloscope. The oscillograms of the discharge voltage and current, as well as of the pulses of laser and scattered probing radiation for the charging voltages U = 14 and 20 kV are presented in Fig. 7.

After the breakdown in the discharge gap at the stage of the current growth, the gradient of refractive index arises due to the increasing concentration of free electrons in the discharge plasma. As a result, the probing beam is deflected, and a certain part of it does not hit the face of the optical waveguide, which leads to the appearance of the first peak of the signal in the oscillogram (Fig. 7c). Its duration (35 ns) approximately equals the first period of the discharge current and is significantly smaller than the total duration of the discharge current (more than 100 ns). Hence, it is possible to state that the decrease in the photodiode signal is caused by the fast reduction of the electron concentration gradient. However, the concentration of electrons in the plasma cannot decrease essentially, because even at low peaking capacitor voltages the current in the discharge gap is rather large. In Refs [8, 9] it was shown both numerically and experimentally that the concentration of electrons in the discharge plasma decreases slower than the amplitude of the discharge current. The authors associate the decrease in the electron concentration gradient with the loss of stability of diffuse phase of the pumping discharge and the transition of the discharge into the inhomogeneous streamer phase with filamentary structure, developed in the central part of the discharge. The small-scale filamentary structure can cause only a small scattering of the probing radiation, which is observed in the experiment.

Stemming from the fact that the distribution of current density and, therefore, the electron concentration N_e, has the shape, similar to that of the distribution of energy input into the discharge plasma, and based on the experimental data, we estimated the refractive index gradient, as well as the electron concentration N_e in the discharge plasma. At the lasing wavelength λ = 308 nm of the XeCl laser the maximal refraction index gradient of the active medium, related to the change of electron concentration, grad n_e, is equal to $\sim 3.48 \times 10^{-6}$ cm^{-1}, while the maximal variation of the refractive index, Δn_e, amounted to $\sim 4.35 \times 10^{-7}$. The corresponding maximal electron concentration of the discharge plasma, calculated using

the formula $N_e = \Delta n_e/(4.46\times10^{-14}\lambda^2)$ [5], is equal to 10^{16} cm^{-3}, where λ is in cm and N_e is in cm^{-3}.

The specific pump power in the laser amounts to ~10 MW cm^{-3} at the energy input ~0.1 J cm^{-3}. In Ref. [9] the theoreticall calculated concentration of free electrons in the the XeCl-laser discharge plasma was equal to $\sim6\times10^{15}$ cm^{-3} for the specific pump power of 6.2 MW cm^{-3} and energy input of 0.3 J cm^{-3}. In Ref. [8] the dynamics of electron density variation in the process of pumping is studied. In accordance with the experimental data [8] at the specific pump power of the XeCl laser ~0.3 MW cm^{-3} and the energy input ~0.07 J cm^{-3} the concentration of free electrons was $\sim10^{15}$ cm^{-3} in the diffuse stage of the discharge, and with the loss of the discharge stability in the presence of a small-scale structure it increased up to $\sim10^{16}$ cm^{-3}.

We associate the second peak of the photodiode signal (Fig. 7c) with gas-dynamic perturbations of the active medium that develop 50–80 ns after the discharge formation. The generation of laser radiation comes to an end before the occurrence of significant gas-dynamic perturbations, so that they have practically no effect on the formation of the radiation field in the cavities of excimer lasers.

To estimate the duration of the development of gas-dynamic perturbations of the active medium in lasers with a 'narrow' discharge at nanoseconds durations of energy input, we used the technique, analogous to that of Ref. [10]. The estimates were performed for the experimentally obtained distribution of the energy input, considered to be instantaneous, under the assumptions, presented in [10]. It was shown that during the time 50–80 ns at the charging voltage $U = 20$ kV the refractive index gradient gradn_{gd} can approach 3.4×10^{-6} cm^{-1}, and at $U = 14$ kV it is equal to 2.1×10^{-6} cm^{-1}. These results sufficiently well agree with the oscillograms in Fig. 7c. Thus, it is possible to state that with respect to the values of refractive index gradient the gas-dynamic optical inhomogeneities in the excimer lasers with a 'narrow' discharge may become comparable with the inhomogeneities of the discharge plasma electron concentration in 50–80 ns from the moment of discharge formation.

3. Conclusions

The results of the study of a repetitively pulsed XeCl laser with a high pulse repetition rate and electrode assembly on the basis of a multiple-section discharge gap with inductance–capacitance discharge stabilisation are reported.

After optimising the pressure of the active mixture of the XeCl laser, the optimal ratio of its components, HCl : Xe : Ne = 2.3 : 19 : 2400 Torr, was found. The width of the discharge at the half-maximum of its glow intensity amounted to ~2 mm

The maximal energy of the laser pulse, 7.9 mJ, was obtained at the charging voltage $U = 22$ kV, and the maximal efficiency coefficient was equal to 1.6% at $U = 14$ kV.

The studies of the repetition rate regime of laser operation were carried out. The limiting repetition rate of radiation pulses appeared to be 5 kHz at the mean laser power 31 W. The mean-square deviation of the pulse energy did not exceed 2.4% at $f \leqslant 5$kHz. These pulse repetition rates were obtained at the velocities of the gas circulation $V \leqslant 18$ m s^{-1} with the purification coefficient of the gas mixture $K = 1.8$.

A shadow technique with photoelectric registration of the optical signal was developed to determine the gas flow velocity in electric-discharge lasers. For the first time the optical inhomogeneity, caused by the acoustic wave, arising in the process of expansion of the gas volume heated within the 'narrow' discharge, was experimentally observed. Using the experimental data the refractive index gradient, associated with the inhomogeneity of free-electron concentration in the discharge plasma of the active medium of the repetitively pulsed XeCl laser with a high pulse repetition rate and 'narrow' discharge, was estimated for the first time, as well as the duration of development of gas-dynamic perturbations in the active medium.

References

1. Goto T., Takagi Sh., Kakizaki K., Sato S., Kosugi Sh., Ohishi T., Kanazawa Y., Ishii A., Teranishi T., Yasuoka K., Shinohe T., Ohashi H., Endo F., Okamura K. *Rev. Sci. Instrum.*, **69**, 1 (1998).
2. Borisov V.M., Vinokhodov A.Yu. Vodchits V.A., Yel'tsov A.V. *Kvantovaya Elektron.*, **30**, 881 (2000) [*Quantum Electron.*, **30**, 881 (2000)].
3. Borisov V.M., Vinokhodov A.Yu. Vodchits V.A., Yel'tsov A.V., Ivanov A.S. *Kvantovaya Elektron.*, **30**, 783 (2000) [*Quantum Electron.*, **30**, 783 (2000)].
4. Andramanov A.V., Kabaev S.A., Lazhintsev B.V., Nor-Arevyan V.A., Selemir V.D. *Kvantovaya Elektron.*, **35**, 311 (2005) [*Quantum Electron.*, 35, 311 (2005)].
5. Andramanov A.V., Kabaev S.A., Lazhintsev B.V., Nor-Arevyan V.A., Pisetskaya A.N., Selemir V.D. *Kvantovaya Elektron.*, **36**, 101 (2006) [*Quantum Electron.*, **36**, 101 (2006)].
6. Andramanov A.V., Kabaev S.A., Lazhintsev B.V., Nor-Arevyan V.A., Pisetskaya A.N., Selemir V.D. *Kvantovaya Elektron.*, **39**, 147 (2009) [*Quantum Electron.*, **39**, 147 (2009)].
7. Andramanov A.V., Kabaev S.A., Lazhintsev B.V., Nor-Arevyan V.A., Selemir V.D. *Kvantovaya Elektron.*, **35**, 359 (2005) [*Quantum Electron.*, **35**, 359 (2005)].
8. Borovkov V.V., Andramanov A.V., Voronov S.L. *Kvantovaya Elektron.*, **26**, 19 (1999) [*Quantum Electron.*, **29**, 19 (1999)].
9. Bychkov Yu.I., Yampol'skaya S.A., Yastremskii A.G. *Kvantovaya Elektron.*, **40**, 28 (2010) [*Quantum Electron.*, **40**, 28 (2010)].
10. Alekhin B.V., Borovkov V.V., Brodskii A.Ya., Lazhintsev B.V., Nor-Arevyan V.A., Sukhanov L.V. *Kvantovaya Elektron.*, **7**, 1516 (1980) [*Sov. J. Quantum Electron.*, **10**, 872 (1980)].